(From D. F. Griffiths, and G. A. Watson, eds., Numerical Analysis Longman, 1986.)

L.N. TREFETHEN

DISPERSION, DISSIPATION, AND STABILITY.

1. INTRODUCTION

Finite difference models are useful only when they are stable. If the von Neumann condition is violated, i.e., some Fourier mode has an amplification factor greater than 1, then the nature of the instability is obvious. But sometimes the von Neumann condition is satisfied and still the model is unstable because of the interaction of distinct Fourier modes — dispersion. The purpose of this paper is to describe such effects. A recurring theme will be the contest between dispersion, which destabilizes, and dissipation, which stabilizes but at some cost in accuracy.

This introductory section will review the basics of dispersion and dissipation, and the remaining sections will present several applications to stability.

Consider the model hyperbolic equation

$$u_t = u_x , \tag{1}$$

and the leap frog (LF) approximation

$$v_j^{n+1} = v_j^{n-1} + \lambda(v_{j+1}^n - v_{j-1}^n) , \tag{2}$$

where $\lambda = k/h = \Delta t/\Delta x$. In Fourier analysis, we insert in (2) a mode

$$v_j^n = e^{i(\omega t + \xi x)} , \qquad x = jh , \quad t = nk , \tag{3}$$

where $\xi \in [-\pi/h, \pi/h]$ is the wave number and $\omega \in [-\pi/k, \pi/k]$ is the frequency, and obtain

$$\text{LF:} \quad \sin\omega k = \lambda \sin\xi h , \tag{4}$$

the dispersion relation for LF. Analogously, the Crank-Nicolson (CN), Lax-Wendroff (LW), and backward Euler (BE) models of (1) have dispersion relations

$$\text{CN:} \quad 2\tan\frac{\omega k}{2} = \lambda \sin\xi h , \tag{5}$$

$$\text{LW:} \quad -i(e^{i\omega k} - 1) = \lambda \sin\xi h + 2i\lambda^2 \sin^2\frac{\xi h}{2} , \tag{6}$$

$$\text{BE:} \quad -i(1 - e^{-i\omega k}) = \lambda \sin\xi h . \tag{7}$$

All of these equations approximate the ideal relationship $\omega = \xi$ for $\xi, \omega \approx 0$.

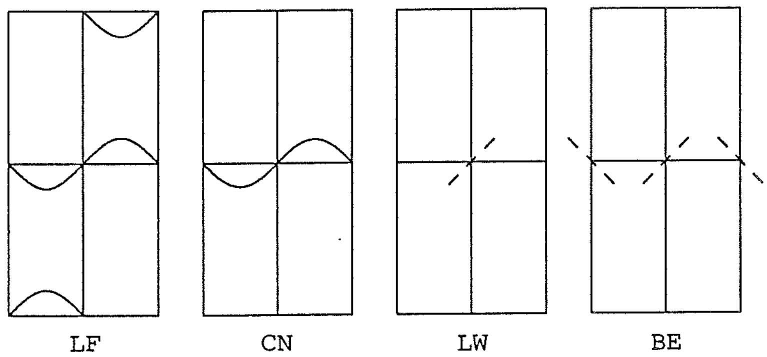

Figure 1. Dispersion relations for four models of $u_t = u_x$.

The relations (4)-(7) are plotted in Figure 1 for $\lambda = \frac{1}{2}$. In each plot the horizontal and vertical ranges are $\xi \in [-\pi/h, \pi/h]$ and $\omega \in [-\pi/k, \pi/k]$, respectively, and thus the domains are rectangles of aspect ratio 2. Alternatively, one could take ξ and ω to be arbitrary and continue the plots periodically in both directions. For LF and CN, ω is real when ξ is real, and the solid curves shown tell the whole story. For LW and BE, ω is real only for isolated values of ξ at the centers of the dashed lines, which are inclined at angles to indicate the (real) values of the derivative $d\omega/d\xi$ there. Elsewhere, ω assumes complex values that are not indicated.

Dissipation is the decay of a Fourier mode as $n \to \infty$ that comes about if $\text{Im}\,\omega > 0$. For a constant-coefficient model of (1), by Parseval's equality, the ℓ^2 norm of $\{v^n\}$ changes with n at a rate precisely determined by the decay of the individual Fourier components (except that the behavior of LF and other multi-level formulas is slightly more complicated). Since $\text{Im}\,\omega = 0$ for all $\xi \in [-\pi/h, \pi/h]$, LF and CN are nondissipative models, while since $\text{Im}\,\omega > 0$ for all nonzero $\xi \in [-\pi/h, \pi/h]$, LW is dissipative. BE, since it dissipates most nonzero modes but not $\xi = \pm\pi/h$, is neither dissipative nor nondissipative.

Dispersion is the interference of Fourier modes that comes about if ξ and ω are related nonlinearly — which they always are, except in unimportant special cases. To quantify this, one can consider the group velocity of a wave packet that consists locally of an oscillation $e^{i(\xi x + \omega t)}$ times a smooth envelope, defined by

$$C = -\frac{d\omega}{d\xi} . \tag{8}$$

For LF, implicit differentiation of (4) leads to the formula

$$C(\xi,\omega) = -\frac{\cos\xi h}{\cos\omega k} . \tag{9}$$

C is the velocity at which energy propagates, as can be made precise by various asymptotic arguments [11]. This is true whenever ξ, ω, and $\frac{d\omega}{d\xi}$ are all real, even though $\omega(\xi)$ may not be real at neighboring values of ξ, as with BE at $\xi = 0$ or $\xi = \pm\pi/h$ [19].

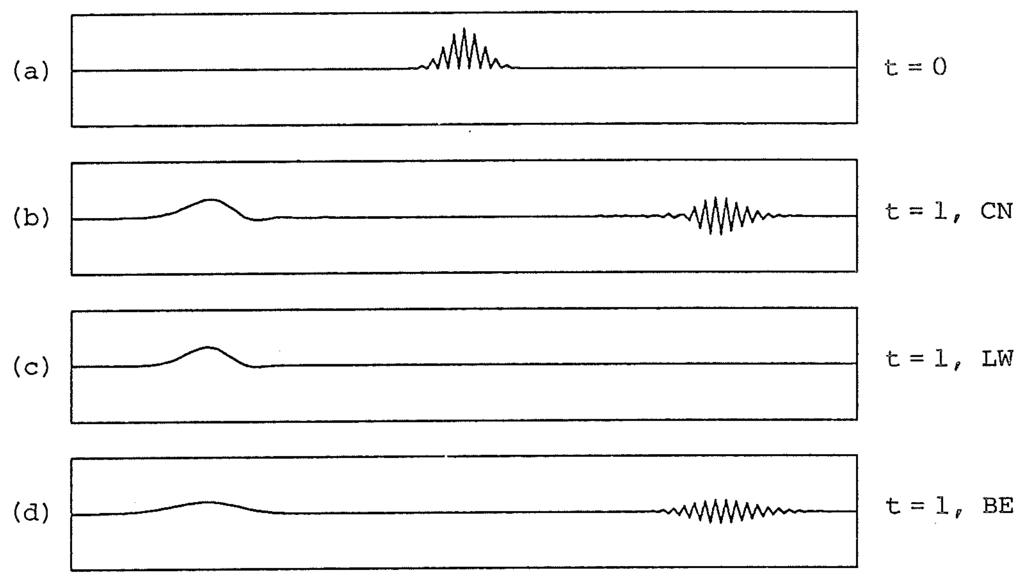

Figure 2. Separation of a wave packet into physical and parasitic components with $C \approx -1$, $C \approx +1$.

Some dispersive phenomena involve sawtoothed Fourier modes with $\xi \approx \pm\pi/h$ and/or $\omega \approx \pm\pi/k$. Figure 2 shows an example computed on the interval [0,3] with $h = .02$ and $\lambda = .5$. At $t = 0$, Figure 2a, the initial signal contains equal amounts of energy at $\xi \approx 0$ and $\xi \approx \pm\pi/h$. Figures 2b-d show the results at $t = 1$ under CN, LW, and BE. In each case about half of the energy has propagated leftward at the correct velocity $C \approx -1$. Under CN and BE, an additional spurious wave packet has also propagated rightward with $C \approx +1$. Such <u>parasitic waves</u> are often generated at boundaries and interfaces, and in nondissipative or weakly dissipative models it is common for them to survive and move in the wrong direction like this. See [5,16,22] for further examples.

Other dispersive phenomena involve Fourier modes with $\xi \approx \omega \approx 0$. To analyze these it is convenient to expand the numerical dispersion relation in a Taylor series in ξ about $\xi = \omega = 0$. In the Lax-Wendroff case (6), for example, one has

$$\omega = \xi\left[1 - \frac{1-\lambda^2}{6}(\xi h)^2 + \frac{i(\lambda-\lambda^3)}{8}(\xi h)^3 + \ldots\right],$$

which corresponds formally to a partial differential equation of infinite order:

$$u_t = u_x + \frac{1-\lambda^2}{6} h^2 u_{xxx} - \frac{\lambda-\lambda^3}{8} h^3 u_{xxxx} + \ldots. \qquad (10)$$

Odd-order derivatives in such an expansion introduce dispersion, and the order of the first nonzero odd derivative of order ≥ 3 is α, the order of dispersion of the difference model. Even-order derivatives introduce dissipation, and the order of the first one is β, the order of dissipation (possibly ∞). The order of accuracy is $\rho = \min\{\alpha,\beta\} - 1$, and is even if $\alpha < \beta$ (dispersion dominates dissipation at low wave numbers) and odd if $\alpha > \beta$ (dissipation dominates dispersion). For LF, CN, LW, and BE we have

LF: $\alpha = 3$, $\beta = \infty$, $\rho = 2$, LW: $\alpha = 3$, $\beta = 4$, $\rho = 2$,

CN: $\alpha = 3$, $\beta = \infty$, $\rho = 2$, BE: $\alpha = 3$, $\beta = 2$, $\rho = 1$.

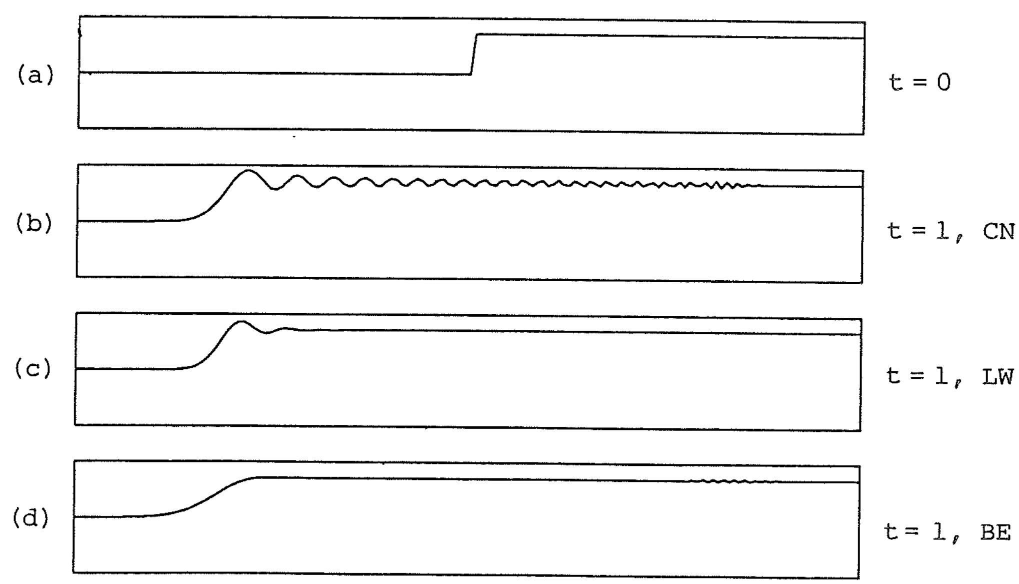

Figure 3. Oscillations around a discontinuity reveal that energy at different wave numbers travels at different group velocities.

To illustrate dispersion and dissipation for $\xi \approx \omega \approx 0$, Figure 3 repeats Figure 2 with new initial data consisting of a step function. At $t=1$, spurious numerical oscillations have developed around the discontinuity under CN and LW. An explanation for this is that energy at various wave numbers $\xi \not\approx 0$ has traveled at corresponding group velocities that are different from the ideal value $C=-1$. Half-way from the origin to the discontinuity, for example, one sees a local wave number under CN corresponding to $C=-.5$. Under LW, such waves have dissipated to nearly zero amplitude, and one has to consider $C \approx -1$ to observe oscillations. Under BE, with $\beta < \alpha$, the dissipation of all modes with $C \neq -1$ is so strong that no oscillations at all are present.

The <u>modified equation</u> for a difference model is the differential equation obtained by deleting from (10) all terms except those of order 1, α, and β, i.e.

$$u_t = u_x + Ah^{\alpha-1}\frac{\partial^\alpha u}{\partial x^\alpha} + Bh^{\beta-1}\frac{\partial^\beta u}{\partial x^\beta} \tag{11}$$

for some A, B [3,23]. This equation suggests that the energy density at wave number ξ will dissipate with time approximately according to

$$\frac{\hat{v}^n(\xi)}{\hat{v}^0(\xi)} \approx \exp(-(-1)^{\frac{1}{2}\beta-1} B\xi(\xi h)^{\beta-1} t) . \tag{12}$$

For an analogous estimate of dispersion, in the case of even-order schemes, we can simplify (11) by dropping the last term. From (8) we then get

$$C(\xi) \approx -1 - (-1)^{\frac{1}{2}\alpha-\frac{1}{2}} \alpha A(\xi h)^{\alpha-1} . \tag{13}$$

Though strictly applicable for dissipative models only if $\xi = 0$, this formula will make good predictions so long as ξ is small enough for the dissipation to be much weaker than the dispersion.

2. <u>STABILITY IN ℓ^p NORMS</u>

Usually stability is measured in the ℓ^2 norm, which is naturally related to amplification factors by Parseval's equality. But for some purposes it is useful to look at other ℓ^p norms, especially ℓ^1 and ℓ^∞, and the situation here is surprising. <u>Any finite difference model of (1) with even order of accuracy is unstable in all ℓ^p norms with $p \neq 2$.</u> This result was proved by Thomée in 1964 (unpublished), and is mentioned on p. 100 of the book by Richtmyer and Morton [14]. By the Lax equivalence theorem, it follows that convergence in ℓ^p cannot occur for arbitrary initial data, although it will still occur if the data are sufficiently smooth.

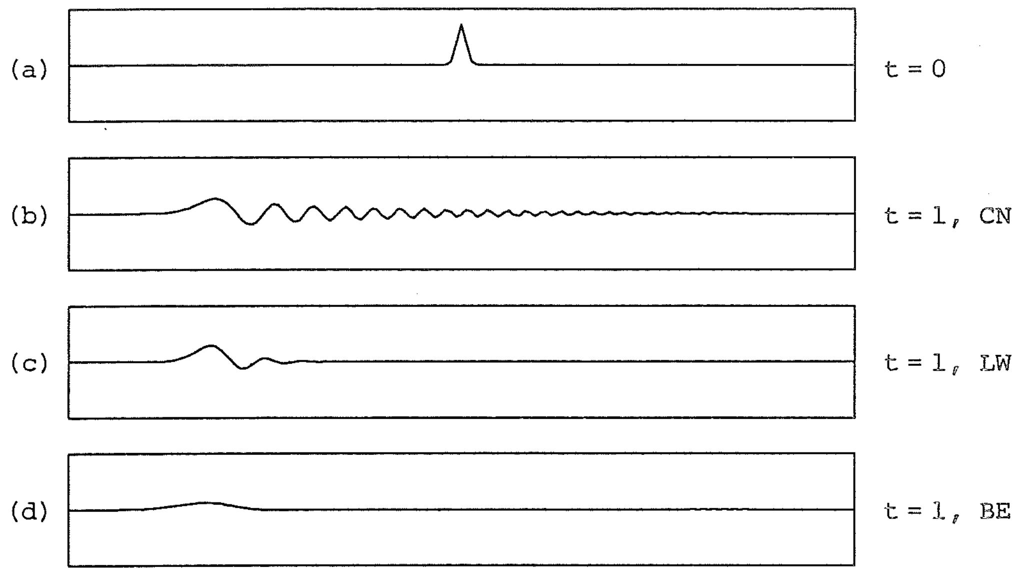

Figure 4. Dispersion of a narrow spike into a train of oscillations explains ℓ^p-instability for $p < 2$. Reversing time explains ℓ^p-instability for $p > 2$.

The explanation is dispersion. To begin with, consider a nondissipative finite difference model ($\beta = \infty$) and initial data consisting of a narrow spike of width $O(h)$ (Figure 4a). As t increases, the wave numbers will separate according to their various group velocities, as they did in Figure 3, resulting in a train of oscillations of width $O(t)$ (Figure 4b). Since $\|v^n\|_2$ is conserved in this process, clearly $\|v^n\|_p$ will increase for each $p < 2$. In fact $\|v^n\|_1$ can grow as fast as $n^{\frac{1}{2}}$, and $\|v^n\|_p$ at the rate $n^{1/p - \frac{1}{2}}$. Since $n \to \infty$ as $h \to 0$ for a fixed time t, this is a mild instability.

On the other hand, suppose we now take as data the wave train of Figure 4b, and integrate further to $t = 2$ with the sign of (1) changed — or equivalently, reverse time and go back to $t = 0$. The result will be an exact recurrence of Figure 4a. In such a process $\|v^n\|_p$ increases for $p > 2$ (up to a limited time), and the rate can be as high as $n^{\frac{1}{2} - 1/p}$. This again is a mild instability.

The same phenomenon causes ℓ^p-instability for dissipative finite difference models of even order ($\alpha < \beta$). If the order of dissipation is β, then by (12), energy at wave number ξ will attenuate on a time scale of order $t \approx h(\xi h)^{-\beta}$, i.e. $n \approx (\xi h)^{-\beta}$. Conversely, significant energy will still be present at step n for wave numbers of order $\xi h \approx n^{-1/\beta}$ and less. By (13), these wave numbers represent a range of group velocities of order $n^{(1-\alpha)/\beta}$, and therefore at step n, the train of oscillations will extend over an interval of length on the order of $(hn)n^{(1-\alpha)/\beta}$, i.e.

$$\boxed{\text{APPROXIMATE WIDTH OF REGION OF OSCILLATIONS: } hn^{\frac{\beta+1-\alpha}{\beta}}} \qquad (14)$$

(This formula predicts oscillations in Figure 3c extending over about 14 grid points, which is about right.) Now suppose the initial pulse was as narrow as possible consistent with containing only wave numbers of order at most $\xi h \approx n^{-1/\beta}$ — that is, it has width of order $hn^{1/\beta}$. Comparing this with (14) gives a broadening by a factor $n^{(\beta-\alpha)/\beta}$ from step 0 to step n, and since the ℓ^2 norm will be approximately conserved, we expect growth in $\|v^n\|_1$ by a factor of order $n^{(\beta-\alpha)/2\beta}$. More generally, for arbitrary p, with a time reversal as before to carry out the argument for $p > 2$, we get

$$\boxed{\text{APPROXIMATE UNSTABLE GROWTH RATE IN } \ell^p \text{ NORM: } n^{\frac{\beta-\alpha}{\beta}\left|\frac{1}{2}-\frac{1}{p}\right|}} \qquad (15)$$

These heuristic arguments, which were given originally in [18], reproduce the results have have been established over the years by rigorous methods of Fourier multipliers and saddle point analysis by Apelkrans, Brenner, Chin, Hedstrom, Serdyukova, Stetter, Strang, Thomée, Wahlbin, and others. In various forms the estimates (14) and (15) have been the subjects of many research papers. For (14), see for example [3,8], and for (15), see the monograph by Brenner, Thomée, and Wahlbin [2]. These authors prove that up to a constant factor, (15) gives precisely the rate of growth of powers of the discrete finite difference solution operator in ℓ^p.

The instability of (15) is weak and will rarely have much practical importance. Among our four examples, with $p = 1$ or ∞, the growth is of order $n^{1/2}$ for LF and CN, $n^{1/8}$ for LW, and n^0 (stability) for BE.

Analogous weak ℓ^p-ill-posedness occurs for hyperbolic partial differential equations in several space dimensions, where geometric focusing effects take the place of the dispersion introduced by discretization. Multidimensional finite difference models are capable of growth in ℓ^p from both sources.

3. STABILITY OF THE INITIAL BOUNDARY VALUE PROBLEM

The last section showed that ℓ^p-instability of finite difference models is caused by dispersion of wave modes with $\xi \approx \omega \approx 0$. This section will show that instability of finite difference models containing boundaries is also a matter of dispersion. This kind of instability is a more serious matter, which causes trouble frequently in practical computations. This time it is the parasitic wave modes with $\xi \approx \pm\pi/h$ and/or $\omega \approx \pm\pi/k$ that are usually responsible.

Consider (1) on the semi-infinite domain $x \geqq 0$, $t \geqq 0$. Mathematically, no boundary condition at $x = 0$ is called for, but a finite difference model will generally require one or more numerical boundary conditions. For example, each of the models LF, CN, LW, and BE requires one numerical boundary condition to determine v_0^{n+1}. The three candidates we will consider are the first-order extrapolation formulas

$$v_0^{n+1} = v_1^n, \qquad v_0^{n+1} = v_1^{n+1}, \qquad v_0^{n+1} = v_2^{n+1}. \tag{16a,b,c}$$

(The last of these is unrealistic and is included for illustration only.) The question is, which combinations of our four difference models with these three boundary conditions are stable, hence will give accurate answers?

A theory of how to answer this question was developed in the period 1960-1972. Naturally one first tries to adapt Fourier analysis, despite the bounded domain, to get a stability criterion analogous to the von Neumann test. The result is known as the Godunov-Ryabenkii stability criterion [14], and amounts to the following for scalar, three-point models of (1): a necessary condition for stability is that the finite difference model — both interior formula and boundary condition — admit no solutions (3) with $\text{Im}\omega < 0 < \text{Im}\xi$. It is clear why a solution of this kind causes instability: it will grow exponentially with the number of time steps. The difference from the von Neumann test is that on the one hand, an unstable mode has to satisfy two equations rather than one, while on the other, the candidates include all waves with $\text{Im}\xi > 0$ rather than just $\text{Im}\xi = 0$. For our twelve difference models, one can verify with a little algebra that there are no unstable modes of this type. So far, so good.

The extension of the Godunov-Ryabenkii criterion to a necessary and sufficient condition for stability was accomplished by Osher and by Kreiss and his colleagues around 1970, and is described in the well-known but difficult "GKS" paper of Gustafsson, Kreiss, and Sundström [7,12]. The essence of the Kreiss-Osher theory is the recognition that there is a second mechanism of instability to worry about: dispersive wave radiation from the boundary. For our scalar problem, the GKS stability criterion is as follows: a necessary and sufficient condition for stability is that the finite difference model admit no solutions (3) with $\mathrm{Im}\omega \leq 0 < \mathrm{Im}\xi$ or with $\xi, \omega \in \mathbf{R}$ and group velocity $C \geq 0$. "Stability" refers here to the rather complicated Definition 3.3 of [7], now commonly called "GKS-stability," but the same criterion gives the right answer for ℓ^2-stability too except in certain borderline cases (mainly $C = 0$ or $\mathrm{Im}\omega = 0 < \mathrm{Im}\xi$).

The GKS criterion reveals that some of our twelve difference models are unstable after all. For example, the wave

$$v_j^n = (-1)^j \qquad (\xi = \pi/h, \quad \omega = 0)$$

satisfies formulas LF, CN, and BE (not LW) and boundary condition (16c). Moreover, for each of LF, CN, and BE, Figure 1 reveals that the corresponding group velocity is $C = 1 > 0$. Therefore LF, CN, and BE are unstable with this boundary condition. To see which of the nine remaining combinations may be stable, if any, we have to check all other admissible combinations of ξ and ω also. For this simple example, that is not as hard as it sounds, and the results are listed in Table 1. Evidently four of the twelve combinations are unstable, and in one case there are two distinct unstable modes.

	LF	CN	LW	BE
(16a)	stable	stable	stable	stable
(16b)	unstable $v_j^n = (-1)^n$	stable	stable	stable
(16c)	unstable $v_j^n = (-1)^j$ or $(-1)^n$	unstable $v_j^n = (-1)^j$	stable	unstable $v_j^n = (-1)^j$

Table 1. Stable and unstable combinations of four interior formulas with three boundary conditions. For the unstable combinations, the unstable normal modes are listed.

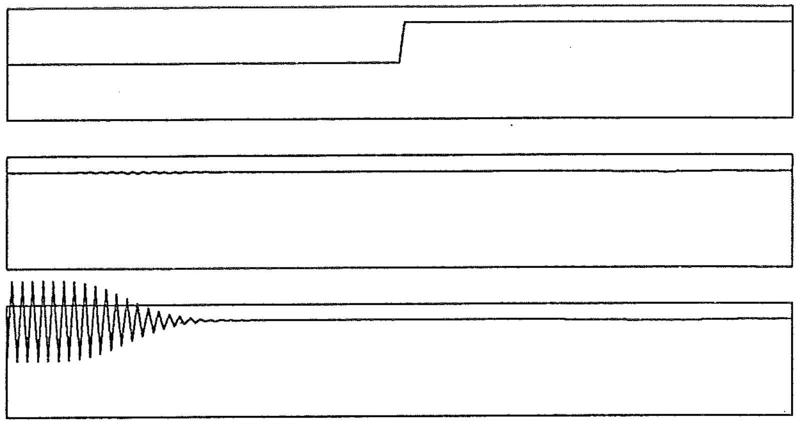

Figure 5. Two computations with formula BE — boundary condition (16b) (stable) and (16c) (unstable).

It is easy to see physically why the modes we have called unstable are troublesome. Figure 5 shows a BE computation with $h = .02$ on the usual interval $[0,3]$ in which the initial distribution is a step function. (At the right-hand boundary the condition is $v \equiv 1$.) For the stable boundary condition (16b), the plot at $t = 2$ reveals that some oscillations have reflected from $x = 0$ into the interior with group velocity $C \approx 1$, but the solution is still approximately right. But with the unstable condition (16c), a spurious wave has been generated at $x = 0$ that will radiate rightwards into the interior forever; nor would decreasing h eliminate it. Convergence to the correct solution will not occur.

It is no coincidence that our only dissipative finite difference model, LW, turned out to be stable with all three boundary conditions. The reason is that dissipation extinguishes the parasitic waves that most often cause instability. For certain classes of problems, dissipativity actually guarantees stability — see [6]. Unfortunately, the guarantee does not extend to many problems of realistic complexity, especially when there are several space dimensions [21]. Also, the weak levels of dissipation used in many practical calculations may prevent instability in theory, but still permit behavior near enough to that of Figure 5c to be troublesome.

Further examples of stable and unstable computations can be found in [17,19,20,21]. The dispersive waves interpretation of the Kreiss-Osher theory is presented rigorously in [19]. Stability of models of initial boundary value problems is a complicated matter, however, especially when systems of equations are involved. Wave radiation from the boundary is still the general mechanism of instability, but testing for the existence of modes of this kind can be very difficult.

4. MULTIPLE BOUNDARIES AND TIME-STABILITY

In finite difference models with several boundaries, waves may bounce back and forth between them, and to understand how this affects stability we must look at reflection coefficients. To begin with, let us return to LF on $x \geqq 0$ with boundary condition (16b) of the last section. For any frequency ω, (4) and (9) (or Figure 1a) show that there are two wave numbers, a "leftgoing" value ξ_L with $C \leqq 0$ and a "rightgoing" value $\xi_R = \pi/h - \xi_L$ with $C \geqq 0$. Let us look for a constant-frequency solution of the form

$$v_j^n = e^{i\omega t}(\alpha e^{i\xi_R x} + \beta e^{i\xi_L x}), \qquad x = jh, \quad t = nk. \tag{17}$$

Inserting (17) in (16b) leads to the equation $\alpha + \beta = \alpha e^{i\xi_R h} + \beta e^{i\xi_L h}$, and since $e^{i\xi_R h} = -e^{-i\xi_L h}$ for $\xi_R = \pi/h - \xi_L$, this reduces to

$$A = \frac{\alpha}{\beta} = \frac{e^{i\xi_L h} - 1}{e^{-i\xi_L h} + 1}. \tag{18}$$

This is the <u>numerical reflection coefficient</u> for the finite difference model. Numerical experiments confirm that if a leftgoing wave at wave number ξ_L hits the boundary $x = 0$, it generates a rightgoing reflection with amplitude given by (18).

Table 1 predicted an unstable mode with $\omega = \pi/k$, $\xi_R = 0$, $\xi_L = \pi/h$. In (18) this mode gives a zero denominator and an <u>infinite reflection coefficient</u>. The existence of an infinite reflection coefficient for some ω always implies GKS-instability, but the converse does not hold, for a zero in the numerator may cancel the zero in the denominator. In fact this happens for the other unstable models of Table 1. In [19] it is shown that under reasonable assumptions, GKS-unstable models exhibit unstable growth in ℓ^2 at a rate at least $\|v^n\|_2 = O(\sqrt{n})$ in general, but at a rate at least $\|v^n\|_2 = O(n)$ if an infinite reflection coefficient is present.

In this section I want to mention two instability phenomena associated not with infinite reflection coefficients, but with <u>finite reflection coefficients greater than 1 in magnitude</u>. It should be emphasized that in a finite difference model with a single boundary, a large finite reflection coefficient (equal to 10, say) will in general not cause instability. The reason is that although a wave that hits the boundary may be amplified by reflection, this happens to it only once, so the resulting growth is bounded. If the model is consistent and GKS-stable, the amount of energy in the incident wave that excites the large reflection will decrease as $h \to 0$, and convergence to the correct solution will occur.

The first multiple-boundary instability phenomenon pertains to hyperbolic equations on a bounded interval. Consider the following example from a recent paper of Beam, Warming, and Yee [1] (see also [5,21]). Let (1) be modeled by BE on the usual interval $[0,3]$. At $x=3$ we impose the boundary condition $v_J^n = 0$, where $J = 3/h$. Inserting the ansatz (17) with x replaced by $x-3$ gives a corresponding reflection coefficient

$$A_R = \frac{\beta}{\alpha} = -1, \tag{19}$$

independent of ω. At $x=0$ we consider both boundary conditions (16a) and (16b). The reflection coefficients $A_L = \alpha/\beta$ are

$$\text{(16a)}: \; A_L = \frac{e^{i\xi_L h} - e^{i\omega k}}{e^{-i\xi_L h} + e^{i\omega k}}, \qquad \text{(16b)}: \; A_L = \frac{e^{i\xi_L h} - 1}{e^{-i\xi_L h} + 1}. \tag{20a,b}$$

Neither of these denominators is ever zero for waves admitted by BE (unlike LF), so each boundary is individually GKS-stable and has finite reflection coefficients. By Theorem 5.4 of [7], it follows that the two-boundary model is GKS-stable too.

Nevertheless, only (16b) is usable in practice for large λ. The attraction of an implicit formula like BE is its applicability to simulations of the steady-state limit $t \to \infty$, because according to von Neumann analysis, the time step can be taken arbitrarily large without causing instability. But Beam, et al. found that when BE is applied with J even and λ large to (1), or to a more realistic problem in transonic gas dynamics, the solutions with (16b) converge as $t \to \infty$ but those with (16a) grow exponentially in t. To illustrate this, Figure 6 shows the solution obtained under BE and (16a) with initial data as in Figure 4, but computed with the large Courant number $\lambda = 300$ ($k = 6$) and plotted at large time intervals $\Delta t = 24$ (4 times steps each). At first, the energy nearly dies away, as it should for the mathematical problem. But a small sawtoothed signal remains that begins to grow unboundedly. Obviously, the steady-state solution $v \equiv 0$ will not be approached as $t \to \infty$.

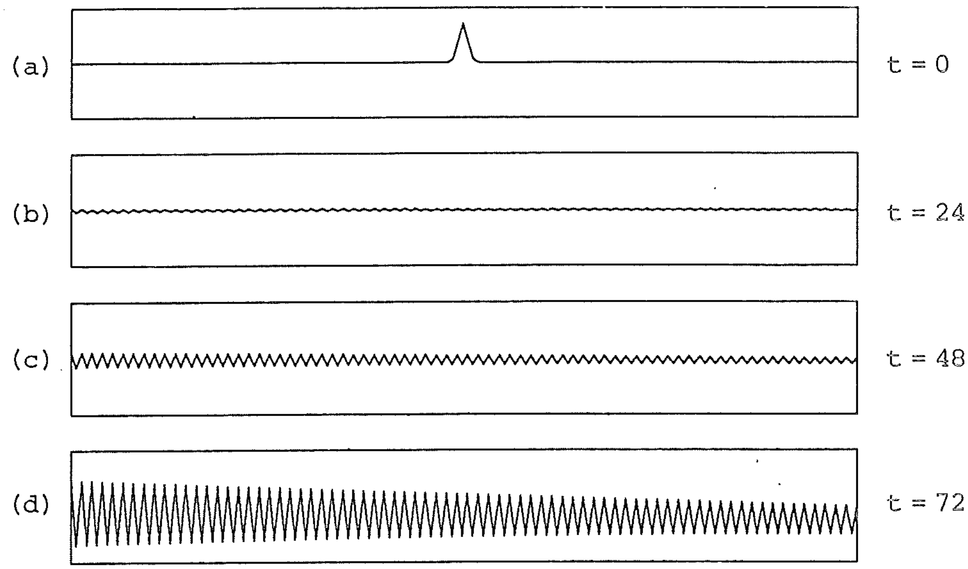

Figure 6. Exponential growth in t caused by repeated reflection between boundaries with a reflection coefficient greater than 1 .

This behavior can be explained by reflection coefficients. For $\lambda \gg 1$, inserting (3) in (7) gives

$$\xi_L = O(1/\lambda) , \qquad \xi_R = \pi/h + O(1/\lambda) ,$$

independently of ω . In particular, these formulas hold for $\omega = \pi/k$. But for that frequency, (20a) gives a large reflection coefficient

$$A_L = O(\lambda) . \tag{21}$$

Now from (19) and (21), we see that a wave may potentially bounce back and forth between the two boundaries, increasing in amplitude by a factor $O(\lambda)$ with each circuit. This will cause growth in any norm at a rate const^t . In Figure 6d, the solution shown is very nearly an eigenmode of the form (17) of the finite difference model with two boundaries. The sawtoothed component, which dominates, is a rightgoing wave that dissipates somewhat as it travels from $x = 0$ to $x = 3$. The fact that the sawtooth is centered below the axis reveals that there is also a nonzero smooth leftgoing component predicted by (19).

By contrast, it can be shown that $\text{Re}(e^{i\xi_L h}) \geq 0$ for all ω with $\text{Im}\,\omega \leq 0$

under BE, and so (20b) implies $|A_L| \leqq 1$. Together with (19), this shows that the two-boundary model with boundary condition (16b) does not admit any solutions consisting of waves that bounce back and forth and increase in amplitude.

Both of these finite difference models are GKS-stable, and will converge to the correct solution as $h \to 0$ for any fixed t . However, the model based on (16a) will fail to converge to anything for fixed h, k as $t \to \infty$. It may also give poor results for finite t with the nonzero values of h used in practice. A finite difference model that admits no exponentially growing solutions as $t \to \infty$ is said to exhibit time-stability (= "practical stability" = "P-stability"). We have illustrated that at least in some cases, time-stability is determined by numerical reflection coefficients.

These arguments can be generalized. Beam, Warming, and Yee consider not just BE but any A-stable time-discretization (including CN) of the usual 3-point difference operator in space, and also space and space-time extrapolation boundary conditions of higher order. For a rigorous analysis of general two-boundary problems by reflection coefficients, see [21]. It is proved there that any two-boundary model with reflection coefficients satisfying $\|A_L\| \, \|A_R\| < 1$ must be time-stable. It is also proved that in the case of a dissipative model, it is enough for an estimate analogous to $\|A_L\| \, \|A_R\| < 1$ to hold for the differential equation. We write norms rather than absolute values for these results since in general, a hyperbolic system or a finite difference model admits several leftgoing and rightgoing modes, and the reflection coefficients imposed by the boundary conditions then give way to reflection matrices.

The second multiple-boundary instability phenomenon of this section is a more speculative idea that I want to mention quite briefly, having to do with hyperbolic equations in a two-dimensional domain with a corner. Suppose a hyperbolic equation is given on $x, y, t \geqq 0$ subject to boundary conditions along $x=0$ and $y=0$, each of which would yield a well-posed problem on a half-plane. (The criterion for well-posedness on a half-plane, due to Kreiss in 1970 [10], is closely analogous to the GKS criterion for stability of a difference model on an interval: the general mechanism of ill-posedness is wave radiation from the boundary, and a problem is always ill-posed if there exists an infinite reflection coefficient at some frequency [9].) Will the problem with the corner be well-posed? This question was first considered by

Osher, and he gave several examples showing that in general the answer is no [13]. The reason is that in some circumstances, a trapped wave packet may bounce back and forth between the two boundaries near the corner, and if its amplitude increases by some finite factor greater than 1 with each reflection, the result will be exponential growth. This may sound like "practical ill-posedness" rather than true ill-posedness. But what makes this problem interesting is that since the wave packet might be arbitrarily close to the corner, the travel time between reflections might be arbitrarily small, and therefore the time constant of such exponential growth cannot be bounded.

In a beautiful paper in 1975, Sarason and Smoller described how to analyze problems like this by invetigating propagation of wave packets along rays [15]. For each frequency ω, the dispersion relation (or characteristic variety) for a differential equation or difference model consists of one or more curves in the wave number space (ξ_x,ξ_y). When a wave packet with parameters (ξ_x,ξ_y,ω) hits the boundary $x=0$, ξ_y will remain constant but ξ_x may jump to another position on this curve, and likewise with the roles of x and y reversed at $y=0$. On the other hand the velocity of propagation of the wave packet in space is given by the vector group velocity $C=-\nabla_\xi\omega$. Given the plot of a dispersion relation, one can apply these considerations to see readily whether the problem in the corner is susceptible to modes that bounce back and forth endlessly between the two boundaries, in which case ill-posedness will occur if the boundary conditions happen to impose large reflection coefficients. On the other hand if all wave packets eventually escape to infinity, the problem is well-posed regardless of the boundary conditions.

Sarason and Smoller showed that for any 2×2 strictly hyperbolic problem — such as the second-order wave equation — the dispersion curves are simply ellipses, leading to the conclusion that all wave packets eventually escape to infinity, so well-posedness is assured. But for finite-difference models, the situation is different, for the dispersion plots are more complicated (see Figure 7 of [16]). It seems certain that one could devise a finite difference model of the wave equation in a corner that was unstable because of repeated reflection at the boundaries. The growth rate would be a catastrophic const^n, despite the well-posedness of the underlying differential equation and the finiteness of all reflection coefficients. This increase in severity from const^t to const^n would be a direct result of the distance between the boundaries becoming vanishingly small at the corner.

It is unlikely that precisely this kind of corner instability ever appears in models of practical interest. But analogous one-dimensional instabilities involving reflections between close together boundaries do occur — see Section 3 of [21].

5. VARIABLE COEFFICIENTS AND NONLINEARITY

In this final section I will mention some ways in which dispersion and dissipation enter into stability questions for problems with variable coefficients or nonlinearity.

The propagation of wave packets under a finite difference model of a linear problem with variable coefficients, such as

$$u_t = a(x) u_x , \tag{22}$$

has been investigated by methods of geometrical optics by Giles and Thompkins [5]. In this situation, even if there is no dissipation, both the amplitude and the wave number of a wave packet change continually in accordance with formulas that depend on the derivative $\frac{da(x)}{dx}$. These changes are numerical artifacts, little related to the behavior of the problem being modeled, and energy is in general not conserved. Giles has made a movie that illustrates the effects of variable coefficients compellingly. In one of its demonstrations, (22) is modeled on an unbounded domain by a nondissipative formula with a variable coefficient $a(x) \leq a_0 < 0$. A numerical wave packet is then observed to oscillate left and right forever between two extreme positions, alternating between smooth and sawtoothed form with each change in direction, even though the differential equation contains no boundaries and admits rightward propagation only.

As an application of these ideas to stability, Giles and Thompkins consider the implications for time-stability of finite difference models with multiple boundaries. In some cases at least, the analysis of the last section can be adapted in a straightforward way. Now, instead of looking for a reflection coefficient bound $\|A_L\| \, \|A_R\| < 1$ to ensure stability, one requires this product to be less than an appropriate frequency-dependent constant. The details are given in [5].

The same principles that govern smoothly varying coefficients also apply to models with smoothly varying mesh spacings. For mesh refinements of a discontinuous sort, on the other hand, it is more appropriate to treat each jump as an interface and look at reflection and transmission coefficients [21].

Another connection of dispersion and dissipation to stability of problems with variable coefficients concerns differential equations on an unbounded domain. When can ℓ^2-stability of a finite difference model of a symmetric hyperbolic system with variable coefficients be inferred from stability of the "frozen" problems for each x ? This question, of obvious practical importance, received much attention in the 1960's, and is discussed in Chapter 5 of the book by Richtmyer and Morton [14]. One result, the Lax-Nirenberg theorem, guarantees stability so long as the coefficients are twice continuously differentiable and the amplification matrix has norm bounded by 1 for each x . A different one, due to Kreiss, guarantees stability when the coefficients are merely Lipschitz continuous provided that the difference model is dissipative and of odd order — that is, $\beta < \alpha$, the same as the condition for ℓ^p-stability in Section 2. Parlett later showed that $\beta \leq \alpha+1$ is good enough in the case of a strictly hyperbolic system such as (22). It would be interesting to know whether the difference between the Lax-Nirenberg and Kreiss-Parlett results can be explained physically in terms of dispersive and dissipative propagation of waves.

When we turn to nonlinear problems, very little is known in a general way about stability. It seems likely that there may be nonlinear stability principles for initial boundary value problems, analogous to the Kreiss-Osher theory of Section 3 for the linear case, that could be obtained by consideration of nonlinear dispersion relations [24], but this has not been investigated. What has been looked at is chiefly the example of the inviscid Burgers equation,

$$u_t = uu_x = (\tfrac{1}{2}u^2)_x , \tag{23}$$

modeled by a leap frog discretization of the form

$$\frac{v_j^{n+1} - v_j^{n-1}}{2k} = (1-\theta)\, v_j^{n+1} \left(\frac{v_{j+1}^n - v_{j-1}^n}{2h}\right) + \theta \left(\frac{(\tfrac{1}{2}v_{j+1}^n)^2 - (\tfrac{1}{2}v_{j-1}^n)^2}{2h}\right) \tag{24}$$

for some $\theta \in [0,1]$. The question of the behavior of (24) dates to Phillips in 1959, and has been studied since then by Stetter, Arakawa, Richtmyer and Morton, Fornberg [4], Kreiss and Oliger, Majda and Osher, Newell, and Briggs, Newell, and Sarie [25]. The omitted references can be found in the papers cited.

For accurate simulation of shock speeds, one might expect that one should take $\theta = 1$, since the model is then in conservation form. But it turns out that $\theta = 2/3$ is also a critical value, at which the energy would be conserved if the time discretization were exact. The papers mentioned show that for $\theta > 2/3$, a 3h-periodic mode of the form $(\ldots,-c,0,c,-c,0,c,\ldots)$ with $c > 0$ will blow up super-exponentially under (24), while for $\theta < 2/3$, the same is true of a mode $(\ldots,c,0,-c,c,0,-c,\ldots)$. Therefore (24) is unstable for all $\theta \neq 2/3$. In computational experiments, however, the explosion is usually observed only in the latter case. The reason is that for $\theta > 2/3$, local patterns approximating the configuration $-c, 0, c$ tend to disperse into waves of constant amplitude radiating in both directions. By contrast, with $\theta < 2/3$, irregular initial oscillations tend to concentrate into the unstable configuration and blow up quickly. (The same also occurs with $\theta > 2/3$ if a boundary with a homogeneous boundary condition is introduced.) Thus (24) seems to be an instance in which dispersion is not the fundamental mechanism of instability, yet it is the factor which controls whether that mechanism is excited.

Finally, consider $\theta = 2/3$ and values of u bounded initially above 0. Either of these conditions is enough to make (24) appear stable in most experiments for short times. Nevertheless, Briggs, et al. discovered that when very many time steps are taken, a fascinating new kind of instability occurs [25]. An example is shown in Figure 7, in which (24) has been applied with $\lambda = \frac{1}{2}$ on the usual grid with periodic boundary conditions. The initial signal is 4h-periodic, except that a random perturbation has been added of amplitude about .01. At $t = 12$, nothing surprising has happened. But at $t = 24$, the signal has begun to undulate in a regular way — an effect one would never encounter in a linear situation. By $t = 36$, the undulations have become dangerously large, and in a few more time steps the CFL limit will be exceeded locally and an explosion will take place. Briggs, et al. show that what is going on is a systematic process of <u>nonlinear focusing</u> of energy, and that this will always occur on any sufficiently fine mesh. The precise positions at which large amplitudes first appear are more or less random, but the nature of their appearance and growth follows a predictable pattern. We conclude that (24) is unstable even for $\theta = 2/3$ and with initial data of one sign.

The lesson of this last example, as of all of the examples of this paper, is that instabilities may have subtle explanations. But they always <u>do</u> have explanations — often related to dispersion of waves.

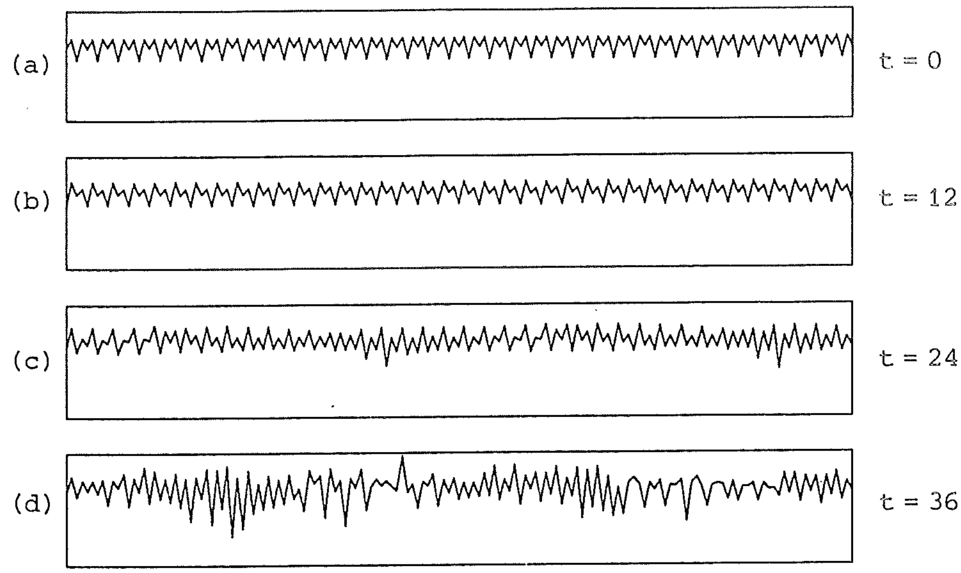

Figure 7. Instability brought about by nonlinear wave focusing in a discrete model of the Burgers equation (after Briggs, Newell, and Sarie).

REFERENCES

1. BEAM, R.M., WARMING, R.F., and YEE, H.C. Stability analysis of numerical boundary conditions and implicit difference approximations for hyperbolic equations, J. Comp. Phys. 48 (1982) 200-222.

2. BRENNER, P., THOMÉE, V., and WAHLBIN, L. Besov Spaces and Applications to Difference Methods for Initial Value Problems, Springer Lect. Notes in Math. v. 434, New York, 1975.

3. CHIN, R.C.Y. and HEDSTROM, G.W. A dispersion analysis for difference schemes: tables of generalized Airy functions, Math. Comp. 32 (1978) 1163-1170.

4. FORNBERG, B. On the instability of Leap-Frog and Crank-Nicolson approximations of a nonlinear partial differential equation, Math. Comp. 27 (1973) 45-57.

5. GILES, M.B. and THOMPKINS, W.T., Jr. Propagation and stability of wave-like solutions of finite difference equations with variable coefficients, J. Comp. Phys., to appear.

6. GOLDBERG, M. and TADMOR, E. Scheme-independent stability criteria for difference approximations of hyperbolic initial-boundary value problems. II, Math. Comp. 36 (1981) 603-626.

7. GUSTAFSSON, B., KREISS, H.-O., and SUNDSTRÖM, A. Stability theory of difference approximations for initial boundary value problems. II, Math. Comp. 26 (1972) 649-686.

8. HEDSTROM, G.W. The rate of convergence of some difference schemes, SIAM J. Numer. Anal. 5 (1968) 363-406.

9. HIGDON, R.L. Initial-boundary value problems for linear hyperbolic systems, SIAM Review, to appear.

10. KREISS, H.-O. Initial boundary value problems for hyperbolic systems, Comm. Pure Appl. Math. 23 (1970) 277-298.

11. LIGHTHILL, J. Waves in Fluids, Cambridge University Press, 1978.

12. OSHER, S. Systems of difference equations with general homogeneous boundary conditions, Trans. Amer. Math. Soc. 137 (1969) 177-201.

13. OSHER, S. Hyperbolic equations in regions with characteristic boundaries or with corners, in Numerical Solution of Partial Differential Equations III, B. Hubbard, ed., Academic Press, New York, 1976.

14. RICHTMYER, R.D. and MORTON, K.W. Difference Methods for Initial-Value Problems, Wiley-Interscience, New York, 1967.

15. SARASON, L. and SMOLLER, J.A. Geometrical Optics and the corner problem, Arch. Rat. Mech. Anal. 56 (1975), 34-69.

16. TREFETHEN, L.N. Group velocity in finite difference schemes, SIAM Review 24 (1982) 113-136.

17. TREFETHEN, L.N. Group velocity interpretation of the stability theory of Gustafsson, Kreiss, and Sundström, J. Comp. Phys. 49 (1983) 199-217.

18. TREFETHEN, L.N. On ℓ^p-instability and oscillation at discontinuities in finite difference schemes, in Advances in Computer Methods for Partial Differential Equations V, R. Vichnevetsky and R.S. Stepleman, eds., IMACS, 1984.

19. TREFETHEN, L.N. Instability of difference models for hyperbolic initial boundary value problems, Comm. Pure Appl. Math. 37 (1984) 329-367.

20. TREFETHEN, L.N. Stability of hyperbolic finite-difference models with one or two boundaries, Proc. AMS-SIAM Summer Seminar on Large-Scale Computations in Fluid Mechanics, AMS, Providence, RI, to appear.

21. TREFETHEN, L.N. Stability of finite difference models containing two boundaries or interfaces, Math. Comp., to appear.

22. VICHNEVETSKY, R. and BOWLES, J.B. Fourier Analysis of Numerical Approximations of Hyperbolic Equations, SIAM, Philadelphia, 1982.

23. WARMING, R.F. and HYETT, B.J. The modified equation approach to the stability and accuracy analysis of finite-difference methods, J. Comp. Phys. 14 (1974) 159-179.

24. WHITHAM, G.B. Linear and Nonlinear Waves, Wiley-Interscience, New York, 1974.

25. BRIGGS, W.L., NEWELL, A.C., and SARIE, T. Focusing: a mechanism for instability of nonlinear finite difference equations, J. Comp. Phys. 51 (1983) 83-106.

L. N. Trefethen
Department of Mathematics
Massachusetts Institute of Technology
Cambridge, Massachusetts 02139
USA